



# Probing Signal-Based Inertia and Frequency Response Estimation for Power Systems with High Penetration of Inverter-Based Resources

## Preprint

Jiangkai Peng,<sup>1</sup> Jin Tan,<sup>1</sup> Przemyslaw Koralewicz,<sup>1</sup> Emanuel Mendiola,<sup>1</sup> Shuan Dong,<sup>1</sup> Anderson Hoke,<sup>1</sup> and Kelsey Horowitz<sup>2</sup>

*1 National Renewable Energy Laboratory*

*2 The AES Corporation*

*Presented at the 2024 IEEE Power and Energy Society General Meeting  
Seattle, Washington  
July 21–25, 2024*

**NREL is a national laboratory of the U.S. Department of Energy  
Office of Energy Efficiency & Renewable Energy  
Operated by the Alliance for Sustainable Energy, LLC**

This report is available at no cost from the National Renewable Energy Laboratory (NREL) at [www.nrel.gov/publications](http://www.nrel.gov/publications).

Contract No. DE-AC36-08GO28308

**Conference Paper**  
NREL/CP-5D00-87925  
August 2024



# Probing Signal-Based Inertia and Frequency Response Estimation for Power Systems with High Penetration of Inverter-Based Resources

## Preprint

Jiangkai Peng,<sup>1</sup> Jin Tan,<sup>1</sup> Przemyslaw Koralewicz,<sup>1</sup> Emanuel Mendiola,<sup>1</sup> Shuan Dong,<sup>1</sup> Anderson Hoke,<sup>1</sup> and Kelsey Horowitz<sup>2</sup>

*1 National Renewable Energy Laboratory*

*2 The AES Corporation*

### Suggested Citation

Peng, Jiangkai, Jin Tan, Przemyslaw Koralewicz, Emanuel Mendiola, Shuan Dong, Anderson Hoke, and Kelsey Horowitz. 2024. *Probing Signal-Based Inertia and Frequency Response Estimation for Power Systems with High Penetration of Inverter-Based Resources: Preprint*. Golden, CO: National Renewable Energy Laboratory. NREL/CP-5D00-87925. <https://www.nrel.gov/docs/fy24osti/87925.pdf>.

© 2024 IEEE. Personal use of this material is permitted. Permission from IEEE must be obtained for all other uses, in any current or future media, including reprinting/republishing this material for advertising or promotional purposes, creating new collective works, for resale or redistribution to servers or lists, or reuse of any copyrighted component of this work in other works.

**NREL is a national laboratory of the U.S. Department of Energy  
Office of Energy Efficiency & Renewable Energy  
Operated by the Alliance for Sustainable Energy, LLC**

This report is available at no cost from the National Renewable Energy Laboratory (NREL) at [www.nrel.gov/publications](http://www.nrel.gov/publications).

Contract No. DE-AC36-08GO28308

**Conference Paper**  
NREL/CP-5D00-87925  
August 2024

National Renewable Energy Laboratory  
15013 Denver West Parkway  
Golden, CO 80401  
303-275-3000 • [www.nrel.gov](http://www.nrel.gov)

## NOTICE

This work was authored in part by the National Renewable Energy Laboratory, operated by Alliance for Sustainable Energy, LLC, for the U.S. Department of Energy (DOE) under Contract No. DE-AC36-08GO28308. This material is based upon work supported by the U.S. Department of Energy's Office of Energy Efficiency and Renewable Energy (EERE) under the Solar Energy Technologies Office Award Number 37772. The views expressed herein do not necessarily represent the views of the DOE or the U.S. Government.

This report is available at no cost from the National Renewable Energy Laboratory (NREL) at [www.nrel.gov/publications](http://www.nrel.gov/publications).

U.S. Department of Energy (DOE) reports produced after 1991 and a growing number of pre-1991 documents are available free via [www.OSTI.gov](http://www.OSTI.gov).

*Cover Photos by Dennis Schroeder: (clockwise, left to right) NREL 51934, NREL 45897, NREL 42160, NREL 45891, NREL 48097, NREL 46526.*

NREL prints on paper that contains recycled content.

# Probing Signal-Based Inertia and Frequency Response Estimation for Power Systems With High Levels of Inverter-Based Resources

Jiangkai Peng, Jin Tan, Przemyslaw Koralewicz,  
Emanuel Mendiola, Shuan Dong, Anderson Hoke  
*National Renewable Energy Laboratory*  
Golden, CO, USA  
jiangkai.peng@nrel.gov, jin.tan@nrel.gov

Kelsey Horowitz  
*The AES Corporation*  
Arlington, VA, USA  
kelsey.horowitz@aes.com

**Abstract**—Power system inertia is the inherent capability of a power system to resist changes in its frequency during disturbances. Real-time inertia estimation technology has become more important due to the low-inertia issues caused by the increasing integration levels of inverter-based resources (IBRs) from renewable energy; however, existing inertia estimation methods hardly consider multiple frequency response controls that act within the same time frame as conventional inertial response, thus making measured inertia values vary under different testing conditions. To resolve this issue, this paper proposes a novel real-time estimation method to simultaneously estimate a power system’s inertia constant and frequency response droop constant using a well-designed probing signal. First, we formulate the inertia and frequency response model of a power system with IBRs. Second, through the integration and manipulation of the developed model, we propose a multivariate linear regression-based estimation method that is resilient to measurement noise. Third, we design a probing signal that can be injected by IBRs to incite the required transients for estimation. Finally, we validate the proposed estimation method through comprehensive power-hardware-in-the-loop experiments using inverter hardware and a realistic island power system model. The results demonstrate that the proposed method can accurately estimate the inertia and droop value of the power system with grid-following IBRs and grid-forming IBRs with virtual synchronous machine control.

**Index Terms**—Frequency response, inertia, inverter-based resources, power-hardware-in-the-loop

## I. INTRODUCTION

Power system inertia plays a crucial role in maintaining grid transient stability and frequency stability by providing time for automatic control to respond and bring the system back to a balanced state. In conventional power systems, inertia is mainly provided by the rotating masses of the synchronous

This work was authored by the National Renewable Energy Laboratory, operated by Alliance for Sustainable Energy, LLC, for the U.S. Department of Energy (DOE) under Contract No. DE-AC36-08GO28308. This material is based upon work supported by the U.S. Department of Energy’s Office of Energy Efficiency and Renewable Energy (EERE) under the Solar Energy Technologies Office Award Number 37772. J. Peng, J. Tan, P. Koralewicz, E. Mendiola, S. Dong and A. Hoke are with National Renewable Energy Laboratory, Golden, CO. (e-mail: Jiangkai.Peng@nrel.gov, jin.tan@nrel.gov). Kelsey Horowitz is with the The AES Corporation, Arlington, VA. (e-mail: kelsey.horowitz@aes.com)

generators (SGs). With the increasing integration levels of renewable energy, fossil fuel-based SGs have been replaced with inverter-based resources (IBRs), such as photovoltaics (PV) and wind. This is expected to have significant implications for the overall dynamics and stability of the power grid because IBRs have fundamentally different dynamical behavior [1].

The inertia challenges for a power system with high levels of IBRs are twofold. First, the increasing integration levels of IBR-interfaced renewable energy sources have resulted in an overall decrease in inertia together with an increase in its variability [2]; thus, online and real-time inertia monitoring is required to ensure the secure and reliable operation of power systems. Second, recent advances in IBR control have enabled IBRs to not only mimic the inertial response of traditional SGs but also provide frequency response faster than traditional SGs. These frequency response controls act within the same time frame as conventional inertial response but with different dynamics, making estimated inertia values inaccurate measures of a power system’s capability to counteract frequency disturbances.

Conventionally, power system inertia is generally estimated by dispatch-based methods [3], [4], where online generator inertia is summed based on the known inertia data of each generator, and event-based methods [5], [6], where the event rate of change of frequency is combined with the confirmed event power change to estimate the inertia; however, dispatch-based methods have accuracy issues because they do not consider IBRs, and event-based methods cannot achieve real-time estimation. To overcome the variability in system inertia caused by IBRs, recently, significant research efforts have been devoted to the development of online and real-time inertia estimation methods. These methods can be generally divided into two categories: ambient signal-based methods and probing signal-based methods. For ambient signal-based methods [7], [8], ambient frequency and power measurements by phasor measurement units are collected to estimate the system inertia based on different methods. For probing signal-based methods [9]–[11], a probing signal disturbance is injected into the power system, and the corresponding frequency measurement

is captured for the inertia estimation.

Nevertheless, existing online and real-time inertia estimation methods [7]–[11] are still based on conventional SG inertial response formulation, where the primary frequency responses are assumed to be negligible. This assumption is valid for conventional power systems, where the frequency response by SG governors is much slower than the inertial response; however, this assumption is being challenged with the increasing integration levels of IBRs. Because the frequency response controls of IBRs are much faster than conventional SG governors, IBRs can act within the same time frame as conventional inertial responses. As a result, the frequency response cannot be decoupled from the inertial response in a power system with high levels of IBRs, making estimated inertia values inaccurate measures of a power system’s capability to counteract frequency disturbances. To resolve this issue, the inertia and frequency response of a power system need to be simultaneously estimated.

To this end, this paper proposes a probing signal-based inertia and frequency response estimation method for power systems with high levels of IBRs. First, we formulate the inertia and frequency response model of a power system with IBRs. Second, through integration and manipulation of the developed model, we propose a multivariate linear regression-based estimation method that is resilient to measurement noise. Third, we design a probing signal that can be injected by IBRs to incite the required transients for estimation. Finally, we validate the proposed estimation method through comprehensive power-hardware-in-the-loop (PHIL) experiments. The main contributions are summarized as follows:

1) We propose a novel real-time online estimation method to simultaneously estimate a power system’s inertia constant and frequency response droop constant using a well-designed probing signal.

2) We validate the performance of the proposed method through comprehensive PHIL experiments using inverter hardware and a realistic island power system model.

## II. INERTIA AND FREQUENCY RESPONSE MODELING

This section introduces the modeling of inertial response and the IBRs’ frequency response.

### A. Inertial Response Modeling

The inertial response of a power system is derived from the synchronous machine swing equation:

$$\frac{2HS_n}{\omega_s} \cdot \frac{d\omega(t)}{dt} + D \cdot \omega = P_m(t) - P_e(t) \quad (1)$$

where  $H$  (MWs/MVA) is the inertia constant,  $D$  (MWs/rad) is the damping coefficient,  $S_n$  (MVA) is the MVA base,  $\omega_s$  (rad/s) is the synchronous speed,  $\omega$  (rad/s) is the angular velocity, and  $P_m$  and  $P_e$  (MW) are the mechanical power input and electrical power output, respectively.

Note that the mechanical power input,  $P_m$ , is related to the frequency response of the power system. For conventional power systems,  $P_m$  is controlled by the generators’ governors;

for IBRs,  $P_m$  is controlled by the IBRs’ frequency controls. Existing inertia methods [7]–[11] generally assume  $P_m$  to be constant immediately after disturbances to simplify the analysis because conventional governors are relatively slow. This assumption is not valid in power systems with high levels of IBRs, where the frequency controls are fast.

### B. IBR Frequency Response Modeling

IBR controls can be generally divided into two categories: grid-following (GFL) and grid-forming (GFM) controls [12]. For GFL IBRs with fast frequency response capabilities, the IBR acts according to the droop characteristics, where it linearly adjusts its output power according to the grid frequency. For GFM IBRs, we consider virtual synchronous generator (VSG) in this paper, which exhibits a combination of inertial and droop characteristics.

Because inertial characteristics has been modeled in the previous section, we consider the frequency response of IBRs specifically as an aggregate linear frequency response (droop) in a short time span after disturbances:

$$P_m(t) = P_m(0) - \frac{K}{2\pi} [\omega(t) - \omega(0)] \quad (2)$$

where  $K$  (MW/Hz) is the aggregate droop constant of all IBRs responding in the inertial time frame.

Therefore, the inertial response of a power system considering the frequency response of IBRs can be obtained by combining (1) and (2) and considering the fact that  $P_m(0) = P_e(0) + D \cdot \omega(0)$  in steady state:

$$\frac{2HS_n}{\omega_s} \cdot \frac{d\omega(t)}{dt} = -\Delta P_e(t) - \left(\frac{K}{2\pi} + D\right) \cdot \Delta\omega(t) \quad (3)$$

where  $\Delta P_e(t) = P_e(t) - P_e(0)$  and  $\Delta\omega(t) = \omega(t) - \omega(0)$ .

It should be noted that damping  $D$  is generally negligible compared to droop  $K$ , thus it is assumed to be 0 in this paper to simplify analysis. The objective of the inertia and frequency response estimation is, therefore, to estimate parameters  $H$  and  $K$  from the  $\omega$  and  $P_e$  measurements after a disturbance based on (3).

## III. PROBING SIGNAL-BASED ESTIMATION METHOD

Using (3) directly for estimation requires the calculation of  $d\omega/dt$ , which is very sensitive to the measurement noise of  $\omega$ ; therefore, we propose the following equation, derived from the integration and manipulation of (3), to reduce the impact of the measurement noise and increase the estimation accuracy:

$$\frac{2HS_n}{\omega_s} \cdot \Delta\omega(t) + \frac{K}{2\pi} \cdot \int_0^T \Delta\omega(t) dt + \int_0^T \Delta P_e(t) dt = 0. \quad (4)$$

where  $T$  is the inertial response measurement data time length.

The three terms in (4)— $\Delta\omega$ ,  $\int \Delta\omega$ , and  $\int \Delta P_e$ —are calculated from the  $\omega$  and  $P_e$  measurements. These terms not only avoid differentiation of measurements but also involve the integration of measurements that can further reduce the impact of the measurement noise.

Further, (4) follows the form  $a_1x_1 + \dots + a_nx_n + b = 0$ , which indicates that the trajectory of its three terms during transients is located on a three-dimensional hyperplane. Consequently, we used multivariate linear regression [13] to simultaneously estimate parameters  $H$  and  $K$ . Here  $K$  represents the aggregate droop constant of all IBRs responding in the inertial time frame.

### A. Probing Signal Design

To produce an accurate estimation using multivariate linear regression, transient frequency measurements,  $\omega$ , and the corresponding electrical power output measurements,  $P_e$ , are needed. Conventionally, these types of measurements are only available after generator tripping events, where the frequency transients ( $\omega$ ) are recorded when a generator with known output power ( $P_e$ ) is suddenly disconnected from the grid.

To facilitate the real-time online estimation, we selected the following probing signal-based method [11], where a 1-MW Hann signal [14],  $P_{\text{probe}}$ , with a 2-s duration is injected into the power system by an IBR to incite the required transients:

$$P_{\text{probe}}(t) = \begin{cases} \cos^2\left(\frac{t-1}{2}\pi\right) & 0 \leq t \leq 2 \\ 0 & \text{else} \end{cases} . \quad (5)$$

As a result, the electrical power output,  $P_e = -P_{\text{probe}}$ , during the probing signal injection and the corresponding frequency transients,  $\omega$ , can be measured.

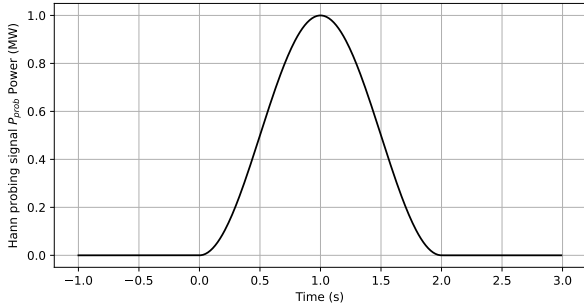


Fig. 1. Hann probing signal.

An illustration of the Hann signal is shown in Fig. 1. It is chosen here because of its pulse-like power profile. It can incite sufficient transients within the power system while minimizing disruptions. Additionally, it is a smooth signal that is easier for IBRs to implement. The overall structure of the proposed probing signal-based inertia and frequency response estimation method is summarized in Fig. 2.

## IV. PHIL EXPERIMENT SETUP

The proposed probing signal-based inertia and frequency response estimation method is validated through PHIL experiments using an island power system model and inverter hardware.

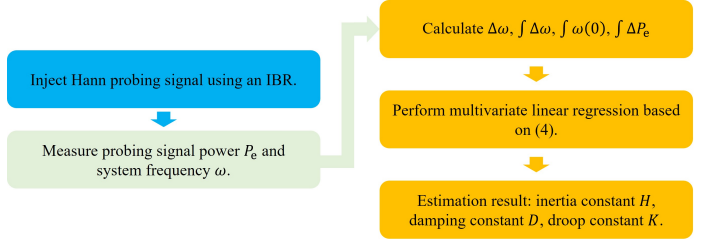


Fig. 2. Probing signal-based inertia and frequency response estimation flowchart.

### A. Kaua'i Island Power System Model

The island power system model is based on the island of Kaua'i in Hawai'i. It is a real-time RSCAD model developed in cooperation with the Kaua'i Island Utility Cooperative (KIUC) that runs in RTDS. The model consists of eight SGs with varied inertia values, two grid-following (GFL) IBRs with fast frequency response capabilities, and one grid-forming (GFM) IBR.

Within the RSCAD model, one GFL IBR is represented via a real-time model with one inverter removed from the plant. The removed inverter is represented via PHIL by the hardware inverter, allowing the power pulses from the real hardware to interact with the real-time model.

### B. PV Plant Hardware

The inverter hardware is a scale replica of a PV plant in Kaua'i. It consists of one DC-coupled PV-battery energy storage system (BESS) inverter, a 400-kW BESS, a 250-kW PV array, and a power plant controller. The PV-BESS inverter is used to inject probing signals into the PHIL test bed, which hosts the power system model. Global Positioning System-synchronized frequency,  $\omega$ , and power,  $P_e$ , measurements are recorded using a medium-voltage data acquisition system [12], [15] with a sampling rate of 500 Hz. These measurements are then processed by the proposed probing signal-based inertia and frequency response estimation method, which is coded in Python. The overall PHIL setup is shown in Fig. 3.

## V. PHIL EXPERIMENT RESULTS

Four PHIL experiment cases are conducted to validate the proposed probing signal-based inertia and frequency response estimation method; this section summarizes the results.

### A. Case I: SGs

This is the base case, with only SGs and no IBRs online (except for the IBR injecting the probing signal). The ground truth inertia of the system can be calculated from the known inertia constants provided by KIUC. The purpose of this case is to benchmark the accuracy of the proposed estimation method on a conventional power system with no IBRs. There are a total of four subcases—A, B, C, and D—with each subcase having a different combination of online SGs and thus different system inertia values.

The injected probing pulse power measurements and the corresponding frequency measurements for Case I-A are



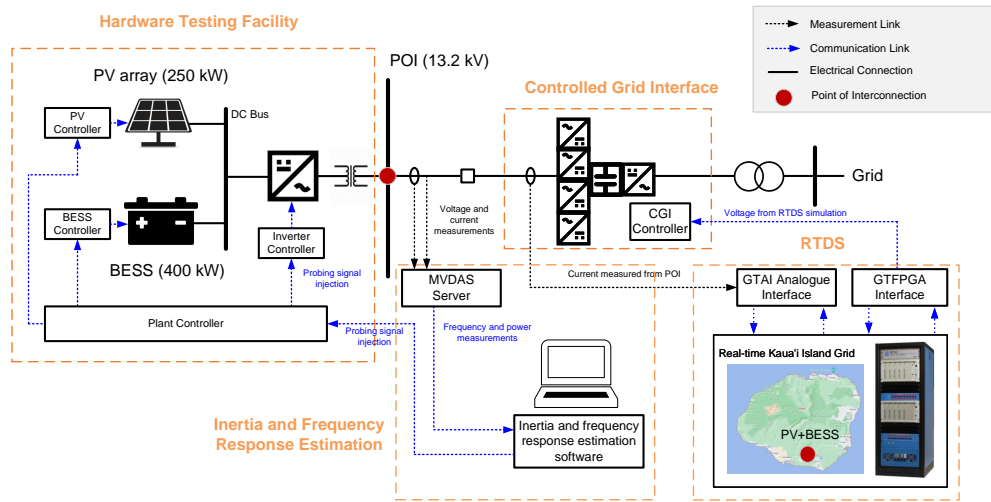


Fig. 3. PHIL experiment setup.

shown in Fig. 4 as an example. It can be observed that the inverter was able to inject the desired Hann probing signal into the grid, and the resulting frequency response is smooth and clean. These measurements are then processed by the proposed estimation method in Python, and the results are visualized in Fig. 5. It can be observed that the trajectory of  $\Delta\omega$ ,  $\int \Delta\omega$ , and  $\int \Delta P_e$  are indeed located on a hyperplane. The estimating results of Case I are summarized in Table I. It is evident that the proposed estimation method was able to accurately estimate the inertia values of the system in all four subcases with an error of less than 5%. Further, note that although the SG governors generally have a slow response speed, they still contribute to a small droop constant,  $K$ , in this case.

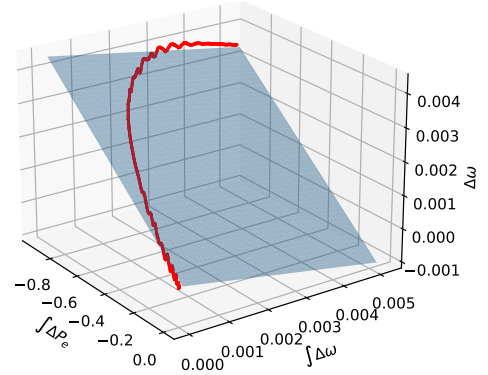


Fig. 5. Multivariate linear regression visualization.

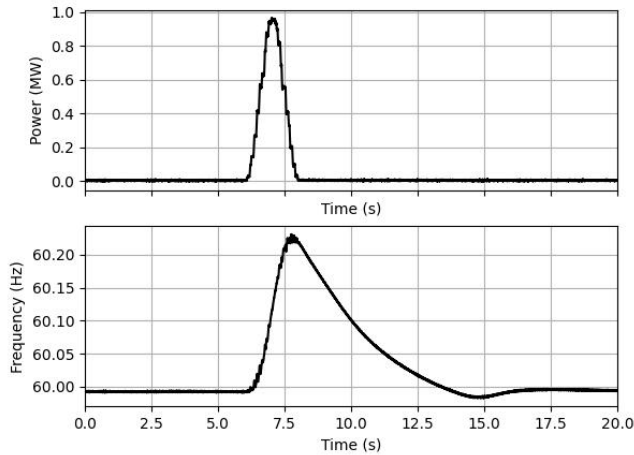


Fig. 4. Probing signal and frequency measurements.

### B. Case II: GFL IBRs

This case has all eight SGs and the two GFL IBRs online. The ground truth inertia of the system is known, and the

TABLE I  
CASE I

	A	B	C	D
Estimated inertia $H \cdot S_n$ (MWs)	103.45	97.78	89.02	82.69
True inertia $H \cdot S_n$ (MWs)	102.05	97.50	90.85	86.35
Inertia estimation error (%)	1.38%	0.28%	-2.01%	-4.24%
Estimated droop $K$ (MW/Hz)	0.71	0.82	1.02	1.21

ground truth droop of the system is calculated from the power-frequency droop control settings of the IBRs. The purpose of this case is to investigate the impact of the GFL IBRs on the accuracy of the proposed estimation method. There are a total of three subcases—A, B, and C—with different IBR droop settings. As shown in Table II, the proposed estimation method was able to accurately estimate the inertia value of the system for all three subcases with an error of less than 10%. Additionally, the proposed method was also able to accurately estimate the droop constant of the GFL IBRs with a an error of less than 3%.

TABLE II  
CASE II

Name	A	B	C
Estimated inertia $H \cdot S_n$ (MWs)	93.80	98.70	103.83
True inertia $H \cdot S_n$ (MWs)	102.05	102.05	102.05
Inertia estimation error (%)	-8.08%	-3.28%	1.75%
Estimated droop $K$ (MW/Hz)	8.52	6.31	3.43
True droop $K$ (MW/Hz)	8.49	6.31	3.51
Droop estimation error (%)	0.46%	-0.03%	-2.64%

### C. Case III: GFM IBRs

This test case has all eight SGs and the one GFM IBR online. The GFM IBR is controlled as a VSG. It has an explicit inertia value and droop constant specified in its controls; therefore, the ground truth inertia and droop of the system are calculated from the VSG control settings. The purpose of this case is to investigate the impact of the GFM IBRs on the accuracy of the proposed estimation method. As shown in Table III, the proposed estimation method was able to accurately estimate the inertia and droop value of the system with the GFM IBR present.

### D. Case IV: SGs and IBRs

This test case has all eight SGs, the two GFL IBRs, and the one GFM IBR online. Similarly, the ground truth inertia and droop of the system are known. The purpose of this case is to validate the accuracy of the proposed estimation method on a system with SGs, GFL IBRs, and GFM IBRs. Again, the proposed estimation method was able to accurately estimate the inertia and droop value of the system, as shown Table III. This validates the performance of the proposed estimation method.

TABLE III  
CASE III AND CASE IV

Name	Case III	Case IV
Estimated inertia $H \cdot S_n$ (MWs)	189.77	182.81
True Inertia $H \cdot S_n$ (MWs)	187.23	187.23
Inertia estimation error (%)	1.36%	-2.36%
Estimated droop $K$ (MW/Hz)	9.11	16.00
True droop $K$ (MW/Hz)	8.78	16.55
Droop estimation error (%)	4.14%	-3.50%

## VI. CONCLUSION

This paper proposed a probing signal-based inertia and frequency response estimation method for power systems with high levels of IBRs. Specifically, the proposed method can simultaneously estimate a power system's inertia constant and frequency response droop constant using a well-designed probing signal injected by IBRs. Comprehensive PHIL experiments have been conducted using inverter hardware and a realistic island power system model. The results demonstrated that the proposed method can accurately estimate the inertia and droop value of the power system with GFL and virtual synchronous generator GFM IBRs.

## ACKNOWLEDGMENTS

We thank Brad W. Rockwell (Kaua'i Island Utility Cooperative) and his team for providing the grid model. We thank AES and GPTech team for providing PHIL testing support and Xinlan Jia (University of Tennessee, Knoxville) for her suggestions on the testing plan. We thank Jarrad Wright (NREL) for his comments on the manuscript. The views expressed in the article do not necessarily represent the views of the DOE or the U.S. Government. The U.S. Government retains, and the publisher, by accepting the article for publication, acknowledges that the U.S. Government retains a nonexclusive, paid-up, irrevocable, worldwide license to publish or reproduce the published form of this work or allow others to do so for U.S. Government purposes.

## REFERENCES

- [1] D. Linaro, F. Bizzarri, D. Del Giudice, C. Pisani, G. M. Giannuzzi, S. Grillo, and A. M. Brambilla, "Continuous estimation of power system inertia using convolutional neural networks," *Nature Communications*, vol. 14, no. 1, p. 4440, 2023.
- [2] E. Heylen, F. Teng, and G. Strbac, "Challenges and opportunities of inertia estimation and forecasting in low-inertia power systems," *Renewable and Sustainable Energy Reviews*, vol. 147, p. 111176, 2021.
- [3] "Inertia: Basic concepts and impacts on the ERCOT grid," 2018. [Online]. Available: [https://www.ercot.com/files/docs/2018/04/04/Inertia\\_Basic\\_Concepts\\_Impacts\\_On\\_ERCOT\\_v0.pdf](https://www.ercot.com/files/docs/2018/04/04/Inertia_Basic_Concepts_Impacts_On_ERCOT_v0.pdf)
- [4] "Future system inertia," 2015. [Online]. Available: [https://eepublicdo wnloads.entsoe.eu/clean-documents/Publications/SOC/Nordic/Nordic\\_report\\_Future\\_System\\_Inertia.pdf](https://eepublicdo wnloads.entsoe.eu/clean-documents/Publications/SOC/Nordic/Nordic_report_Future_System_Inertia.pdf)
- [5] D. Zografos and M. Ghandhari, "Estimation of power system inertia," in *2016 IEEE Power and Energy Society General Meeting (PESGM)*. IEEE, 2016, pp. 1–5.
- [6] D. Zografos, M. Ghandhari, and R. Eriksson, "Power system inertia estimation: Utilization of frequency and voltage response after a disturbance," *Electric Power Systems Research*, vol. 161, pp. 52–60, 2018.
- [7] "Effective inertia," 2020. [Online]. Available: [https://www.naspi.org/sites/default/files/2021-04/DIS1\\_01\\_farantatos\\_epri\\_naspi\\_20210413.pdf](https://www.naspi.org/sites/default/files/2021-04/DIS1_01_farantatos_epri_naspi_20210413.pdf)
- [8] K. Tuttleberg, J. Kilter, D. Wilson, and K. Uhlen, "Estimation of power system inertia from ambient wide area measurements," *IEEE Transactions on Power Systems*, vol. 33, no. 6, pp. 7249–7257, 2018.
- [9] "Inertia and system strength measurement and analytics," 2021. [Online]. Available: <https://www.pjm.com/-/media/committees-groups/forums/emerging-tech/2022/20220614/item-4---renewable-integration---inertia-system-strength-measurements-and-analytics.ashx>
- [10] N. Hosaka, B. Berry, and S. Miyazaki, "The world's first small power modulation injection approach for inertia estimation and demonstration in the island grid," in *2019 8th International Conference on Renewable Energy Research and Applications (ICRERA)*. IEEE, 2019, pp. 722–726.
- [11] Z. Jiang, H. Yin, H. Li, Y. Liu, J. Tan, A. Hoke, B. Rockwell, and C. Kruse, "Probing-based inertia estimation method using hybrid power plants," in *2023 IEEE Power & Energy Society General Meeting (PESGM)*. IEEE, 2023, pp. 1–5.
- [12] A. Hoke, P. Koralewicz, R. W. Kenyon, B. Wang, L. Yu, K. Kawamura, and J. Tan, "Stabilizing inverter-based transmission systems: Power hardware-in-the-loop experiments with a megawatt-scale grid-forming inverter," *IEEE Electrification Magazine*, vol. 10, no. 3, pp. 32–44, 2022.
- [13] D. A. Freedman, *Statistical models: theory and practice*. cambridge university press, 2009.
- [14] O. M. Essenwanger, *Elements of statistical analysis*. The Netherlands: Elsevier, 1986.
- [15] S. D. Shah, P. J. Koralewicz, V. Gevorgian, and R. B. Wallen, "Impedance measurement of wind turbines using a multimegawatt grid simulator," National Renewable Energy Lab.(NREL), Golden, CO (United States), Tech. Rep., 2019.